Holographic Localization of Passive UHF RFID Transponders

Robert Miesen, Fabian Kirsch, Martin Vossiek
Institute of Electrical Information Technology
Clausthal University of Technology
D-38678 Clausthal-Zellerfeld, Germany
miesen@iei.tu-clausthal.de

Abstract— **In this paper a method for holographic localization of passive UHF-RFID transponders is presented. It is shown how persons or devices that are equipped with a RFID reader and that are moving along a trajectory can be enabled to locate tagged objects reliably. The localization method is based on phase values sampled from a synthetic aperture by a RFID reader. The calculated holographic image is a spatial probability density function that reveals the actual RFID tag position. Experimental results are presented which show that the holographically measured positions are in good agreement with the real position of the tag. Additional simulations have been carried out to investigate the positioning accuracy of the proposed method depending on different distortion parameters and measuring conditions. The effect of antenna phase center displacement is briefly discussed and measurements are shown that quantify the influence on the phase measurement.**

Keywords-holography; synthetic aperture radar; phase measurement; position measurement; radio frequency identification; UHF RFID; transponder

I. INTRODUCTION

RFID technology is in constant development since it was introduced by the British army in the 1940s [1]. Especially UHF RFID systems have become popular because of their relatively large reading range. As the number of simultaneously identifiable tags grows with increasing reading range, the spatial information of each individual tag becomes more valuable. In warehouse applications, fixed gate readers are commonly applied to monitor the passage of tags and even distinguish between passing tags and stray tags in the vicinity of the gate. However, very often e.g. in stock inventory systems not only the tag identity but also the position information is crucial. Mobile readers are employed in various applications. Attached to vehicles or persons readers are moved in environments with numerous detectable tags. If multiple tags cannot be distinguished, or if an identified tag cannot be located the benefit of the RFID system is severely reduced.

Many RFID readers perform fully coherent demodulation of the tag signal and recover the signal phase information. The phase information can be evaluated and utilized in several ways to enhance the RFID systems capability [2]. Simple information like the moving direction of a tag when it passes a gate can be extracted or spatial information about the tag position relative to the reader can be derived. A summary of current methods can be found in [3]. Improved frequency domain phase difference of arrival based approaches as described in [4] are a current research topic. However, most multi-frequency considerations were done under US regulations which provide a relatively large bandwidth to Gen 2 UHF RFID systems. In the EU the bandwidth between the four main channels is limited to 1.8 MHz. As shown in [5] noise strongly affects measurements with small frequency offsets.

A method to compensate unknown tags properties is presented in [6]. Further work on localization of passive UHF RFID utilizing the FMCW principle is described in [7] and has been investigated on 2.45 GHz passive tags in [8]. A combination of phase measurement and FMCW distance measurement is described in [9]. In [10] it was shown that UWB ranging in passive UHF RFID is an option to mitigate multipath distortions. For fixed readers, antenna arrays can be utilized to determine tag locations as presented in [11, 12].

Holographic methods are well known in the area of ultrasonic and radar imaging [13-15]. Recently, such methods are also used to localize active transponders based on broadband measurement signals [16]. In contrast to the approaches mentioned above, the presented method does not require any changes in tag, reader and antenna hardware as recent UHF readers offer the phase readout option required for our approach. In this paper we present a single frequency, narrowband holographic method to localize passive UHF RFID tags.

Section II gives a comprehensive explanation on how the phase information of modulated backscatter transponders is retrieved. In section III we present the proposed method. Measurement results are described in section IV. In section V simulated data is utilized to consider the effects of distorted input data on the localization quality. In section VI we investigate the phase distortion effects of directional planar antennas on the measurements. Section VII gives a conclusion and an outlook on further research directions.

II. PHASE MEASUREMENT

As stated before, a fully coherent demodulation is necessary to recover the phase information required for CW radar based

Most of the work presented in this paper has been sponsored by the companies BILSTEIN GmbH & Co. KG, Hagen, Germany, Rheinzink GmbH, Datteln, Germany and Wuppermann AG, Leverkusen, Germany and Symeo GmbH, Munich Germany within the steel and mining research cluster Auto-ID (MonLAID) of Clausthal University of Technology

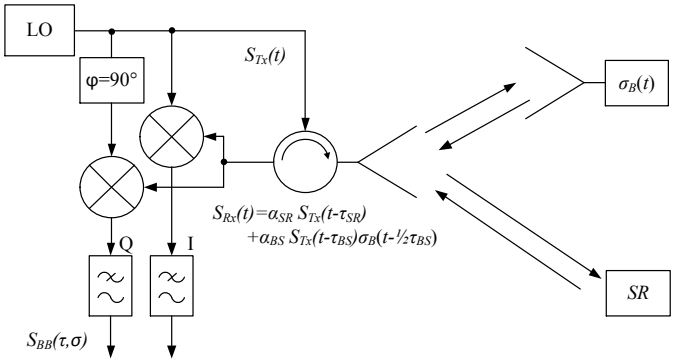

Figure 1. Block diagram of sensor and backscatter transponder.

ranging approaches. The backscatter transponder principle is well-known [17]. Several methods for CW ranging and identification of backscatter transponders are presented in [18]. Fig. 1 shows a block diagram of a basic backscatter transponder reader system.

Let us assume that the transmitted signal of the reader is given by:

$$s_{Tx}(t) = \cos(\omega_c t + \varphi_0)\,, \tag{1}$$

where ω_c and φ_0 are the carrier frequency of the reader and the initial phase offset. Given a RFID tag data signal denoted by *data(t)*, the modulation of the tag can be written as:

$$\sigma_B(t) = \begin{cases} \sigma_0 & if\ data(t) = 0 \\ \sigma_1 & if\ data(t) = 1 \end{cases}, \tag{2}$$

with the two unknown complex valued modulation states of the backscatter transponder given as:

$$\sigma_{0,1} = \sigma_{I,0,1} + j \cdot \sigma_{Q,0,1}\,. \tag{3}$$

The received signal S_{Rx} consists of the reader signal reflected and modulated by the backscatter transponder denoted by BS and $i = 1\ldots N$ reflections from static reflectors denoted by SR. Hence we get:

$$\begin{aligned} S_{Rx}(t) &= \alpha_{BS} \cdot S_{Tx}(t-\tau_{BS}) \cdot \sigma_B(t-\frac{1}{2}\tau_{BS}) + \\ &\sum_{i=1}^{N} \alpha_{SR,i} \cdot S_{Tx}(t-\tau_{SR,i}) \end{aligned}\,. \tag{4}$$

α_{BS}, α_{SR} and τ_{BS}, τ_{SR} denote the amplitude and round-trip time of flight values of the partial echoes. For the sake of simplicity only one static reflector and no multipath reflections are considered to reveal the basic phase relations.

After IQ demodulation and lowpass filtering the complex baseband signal can be written as

$$\begin{aligned} \vec{S}_{BB} &= \alpha_{SR} \begin{pmatrix} \cos(\omega_c\tau_{SR}) & -\sin(\omega_c\tau_{SR}) \\ \sin(\omega_c\tau_{SR}) & \cos(\omega_c\tau_{SR}) \end{pmatrix} \cdot \begin{pmatrix} 1 \\ 0 \end{pmatrix} + \\ &\alpha_{BS} \begin{pmatrix} \cos(\omega_c\tau_{BS}) & -\sin(\omega_c\tau_{BS}) \\ \sin(\omega_c\tau_{BS}) & \cos(\omega_c\tau_{BS}) \end{pmatrix} \cdot \begin{pmatrix} \sigma_I \\ \sigma_Q \end{pmatrix} \end{aligned}\,. \tag{5}$$

The vector $(1,0)^{\mathrm{T}}$ represents the static reflector as the signal is not modulated. If we calculate the difference of the signal from two different modulation states σ_0 and σ_1 we get:

$$\begin{aligned} \Delta S_{BB,\mathrm{mod}} &= \alpha_{BS} \begin{pmatrix} \cos(\omega_c\tau_{BS}) & -\sin(\omega_c\tau_{BS}) \\ \sin(\omega_c\tau_{BS}) & \cos(\omega_c\tau_{BS}) \end{pmatrix} \cdot \\ &\begin{pmatrix} \sigma_{I,1} - \sigma_{I,0} \\ \sigma_{Q,1} - \sigma_{Q,0} \end{pmatrix} \end{aligned}\,. \tag{6}$$

Equation (6) shows that only the distance dependent terms of the backscatter transponder remain. The vector $\Delta S_{\mathrm{BB,mod}}$ is rotated around the origin of the IQ-plane depending on the round-trip time of flight τ_{BS}. I and Q values of $S_{\mathrm{BB}}(\tau,\sigma)$ can be recovered for both modulation states of the backscatter transponder. Phase information solely depending on the distance between antenna and backscatter transponder can therefore be derived via digital post processing.

III. Localization Method

Throughout this paper we consider 2D scenarios where the reader antenna and the tag are located in the same plane. The method can easily be extended to 3D.

The antenna is moved along a known trajectory. Phase measurements in respect to one or more transponders are made at multiple positions $(x_{\mathrm{a,m}}, y_{\mathrm{a,m}})$, $m = 1\ldots N$ on the trajectory. The distance between reader and tag and thus the baseband signal phase $\varphi_m(x_a, y_a, x_t, y_t)$ can be calculated as:

$$\begin{aligned} \varphi_m(x_a, y_a, x_t, y_t) &= \frac{2\pi}{\lambda_c} 2d_{a,t} \bmod 2\pi = \\ &\frac{2\pi}{\lambda_c} 2\sqrt{(x_a - x_t)^2 + (y_a - y_t)^2} \bmod 2\pi \end{aligned}\,, \tag{7}$$

where x_{a} and y_{a} denote the x- and y-position of the reader antenna. x_{t} and y_{t} denote the x- and y-position of a specific tag. λ_{c} is the wavelength of the carrier frequency.

For every point of the image a hypothesis is created. All measured phase values would originate in this point, if the assumed position represented in the image point is equal to the tag position. From this it follows that the N measured phase values $\varphi_m(x_a, y_a, x_t, y_t)$ at the positions $x_{\mathrm{a,m}}$, $y_{\mathrm{a,m}}$ have to match the values calculated using equation (7). Now, the measured phase values $m = 1\ldots N$ are used to reconstruct the signals at the point of the hypothesis. The summation of these signals represents the likelihood of the tag being located at the assumed position. By adding these signals coherently a spatial matched filtering is realized. At a point near the tag position the sum grows as the signals superimpose constructively. At

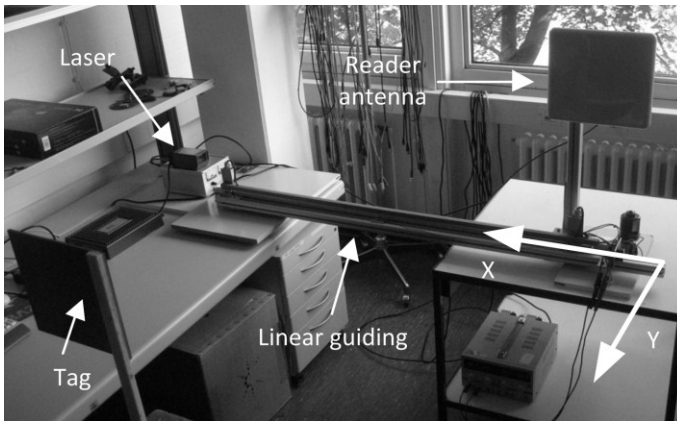

Figure 2. Measurement setup with reader antenna mounted on a movable linear guiding. The tag faces the reader antenna. A laser system has been used to determine the reader antenna position.

positions distant to the tag the signals superimpose at random phase angles and the sum is significantly lower than at or near the tag position. This approach is represented in the probability function,

$$P(x_i, y_i) = \left| \sum_{m=0}^{n} A_m e^{j\left(\frac{4\pi d_{im}}{\lambda} - \varphi_m\right)} \right|, \qquad (8)$$

where (x_i, y_i) denotes the coordinate of an image point, d_{im} denotes the distance between the image point and the aperture point m and φ_m denotes measured phase values. A_m is the amplitude of the measured signal. As a result of the severe multipath environment the measured signal amplitude is notably distorted, as shown in Fig. 4. Therefore, the amplitude is not used in the reconstruction and A_m is set to 1.

This method can easily be extended to 3-dimensional localization by calculating the distance d_{im} in three dimensional space and extending the probability function (8) to $P(x_i, y_i, z_i)$. To obtain a resolution not only in the xy-plane but also in z-direction (i.e. hight) a spatial distribution of the aperture trajectory in z-direction is required. If a moving vehicle generates the synthetic aperture in lateral direction, an upright 1D antenna array attached to the vehicle can be used to create the aperture component in z-direction.

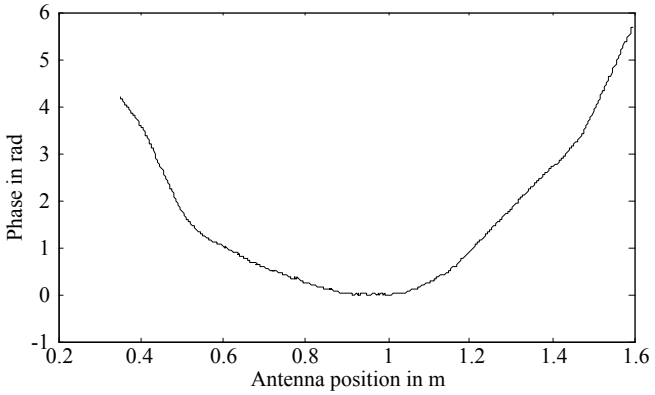

Figure 3. Measured phase data.

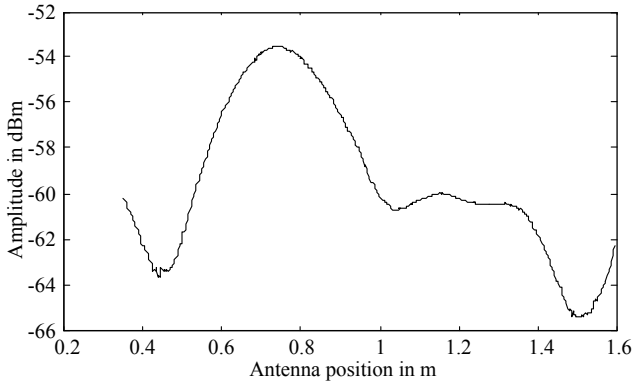

Figure 4. Measured signal amplitude.

The position of the tag can be unambiguously calculated from phase measurements taken from three different locations. In the ideal case all three signals will superimpose at exactly the same phase angel in a single point. This is very similar to the spatial domain phase difference of arrival method described in [3]. Two independent angles of arrival can be derived from three phase measurements. Via basic geometry the position of the tag can be constructed. The advantage of the proposed holographic method is that it is a probabilistic approach that uses all available phase values coherently. By this, the effect of multipath errors and of outliers is effectively reduced.

IV. Measurement Results

Measurements were carried out in a lab/office environment with metal structures of tables and shelves as well as metal ceiling structures. No special precaution has been taken with respect to the propagation qualities of the environment. The test setup is shown in Fig. 2. The Antenna is moving on a straight line at $y_a = 0$ as depicted in Fig. 2.

The minimal distance between tag and antenna is $y_t = 1.5$ m at the antenna position of $x_a = 0.9$ m. The antenna was directed to the tag at the position of minimum distance. The measured phase values are shown in Fig. 3. The multipath fading caused by the reflective environment can be seen easily from the deformation of the curve. The distortion caused by the environment is also visible in the received signal strength shown in Fig. 4.

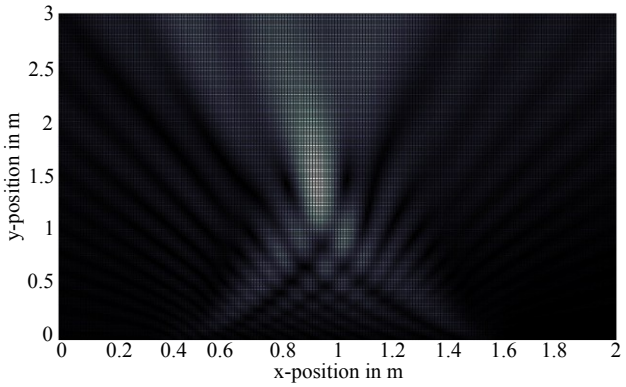

Figure 5. Holographic image calculated from the entire measurement data.

TABLE I. PARAMETERS OF HOLOGRAPHIC RECONSTRUCTIONS AND RESULTING LOCALIZATION ERRORS

No.	Step width in m	Aperture length in m	Localization error x in m	Localization error y in m
1	0.002	1.243	+0.02	-0.07
2	0.017	1.243	+0.02	-0.08
3	0.002	0.621	+0.03	-0.11
4	0.017	0.311	+0.06	-0.02
5	0.040	0.311	+0.05	+0.17

The maximum signal strength is varying rather independently from the distance between tag and reader antenna.

Utilizing (8) a holographic image of the area is calculated. The image size is 2 m by 3 m. The resulting image is shown in Fig. 5. The pixel size of the image was chosen as 1 cm. The maximum of the resulting image represents the actual tag position which is located at $x_t = 0.92$ m and $y_t = 1.43$ m. The determined position matches the real position mentioned above very well. The length of the aperture is 1.24 m. 587 phase measurements have been taken, thus the distance between two successive measurements on the trajectory is 0.002 m.

To investigate the impact of the length and discretization of the aperture, holographic images have been calculated for different subsets of the measurement data. Table 1 shows the applied parameters and the resulting errors of the calculated tag position in x- and y-direction. An increase of the aperture discretization step width by a factor of 8 with a constant length of the aperture does not show any significant impact. Reducing the aperture length to 0.62 m leads to a decreased lateral resolution and the position of the maximum is slightly varied. The change can be seen in Fig. 6.

In a further experiment the aperture discretization step width was increased again by a factor of 8 and the aperture length has been decreased to 0.31 m. The resulting image is displayed in Fig. 7. The main maximum area grows notably while the position of the maximum remains close to the real tag position. The holographic image obtained with parameter set no. 5 of Table 1, was calculated from only 8 measurement values. The error in y-direction increases notably. But even in this unfavorable condition the localization result differs only 18 cm from the real tag position.

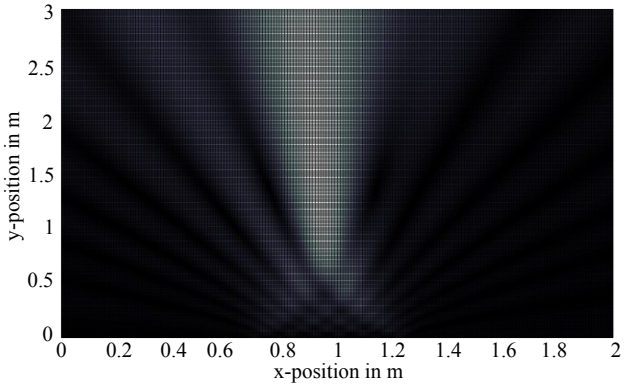

Figure 6. Holographic image of parameter set no. 3.

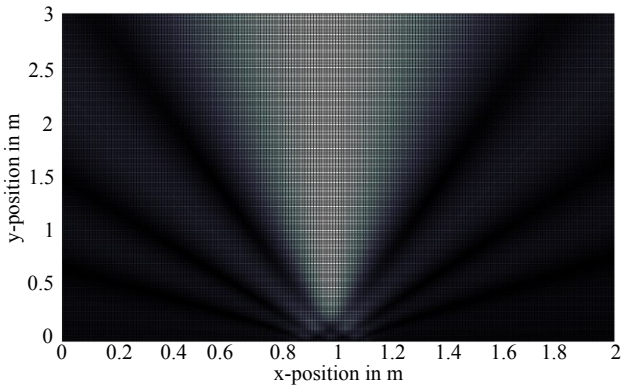

Figure 7. Holographic image of parameter set no. 4.

V. DISTORTION ANALYSIS

Simulations have been carried out to validate the measurement data. Fig. 8 shows simulated phase data of a tag positioned at $x_t = 0.9$ m and $y_t = 1.5$ m, in respect to the antenna moving from $x_a = 0.35$ m to $x_a = 1.55$ m at $y_a = 0$. A holographic image has been calculated from this data utilizing (8) and is shown in Fig. 9. The maximum value of the image is as expected at the position of $x_t = 0.90$ m and $y_t = 1.50$ m. Compared to the image of the measurement data the simulation result is slightly sharper and the main maximum does not blur at the top left side. The deviation between the measurement data and the simulated data has been investigated and is shown in Fig. 10. The measurement data is in good agreement with the simulated data. The mean value of the data shown in Fig. 10 is 0.02 rad and the standard deviation is 0.23 rad. It was observed that the deviation of the same measurement setup in different runs is very similar and very likely a result of the reflective environment. It is well known that multipath propagation is one of the major problems in local positioning systems [19].

The phase error has been simulated with random distributions adjusted to the characteristics of real measured data. However the investigated phase error maxima range from $-\pi$ to $+\pi$ which is notably bigger than for the measured values.

A number of 1000 simulations with random phase

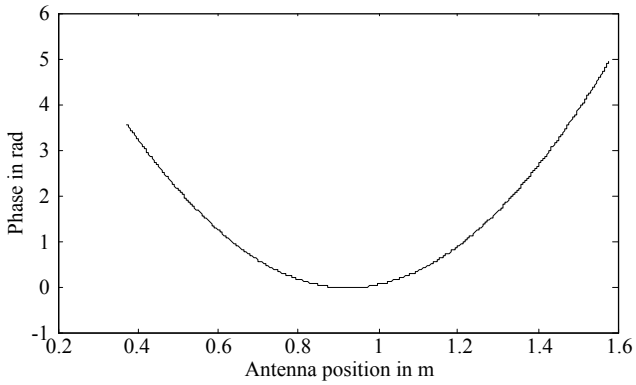

Figure 8. Simulated phase data.

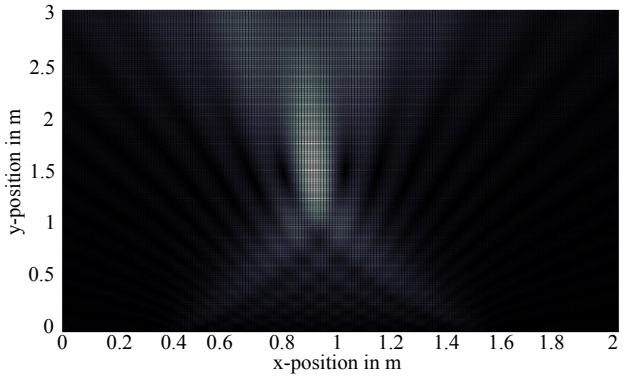

Figure 9. Holographic image resulting from ideal simulated data.

deviations have been carried out to study the deviation of the calculated tag position with respect to the quality of the measurement data. The results are presented in Fig. 11. Both, the error in x-direction and in y-direction follow a Gaussian distribution. The distribution is visible in the histogram of the y-error. Considering the geometric condition it is evident that the precision in radial direction (i.e. y-direction) is much worse than the lateral precision. Only a movement lateral to the wave propagation direction contributes to the image resolution for a monofrequent holography [13]. For a curved trajectory that covers an angle of 90 degree or more, the x- and y-uncertainty would be uniformly distributed.

The width of the bins is limited by the discretization of the image that is 1 cm in our case. Therefore the distribution of the x error with a mean value at x = -0.0013 m and a standard deviation of 0.023 m is very narrow. Both distributions match the shape of the main maximum area of the holographic image. The distributions of the errors show that the holographic method is stable in terms of the applied erroneous input data.

VI. Antenna Phase Response

In the measurements described above a standard UHF-RFID antenna has been used. RFID reader antennas are usually strongly directive. During a movement of the antenna the antenna changes its angular orientation to the tag. As the antenna pattern is not symmetric the measured phase values are varied by the angle of sight due to antenna phase center deviations. The phase center of an antenna can be described as

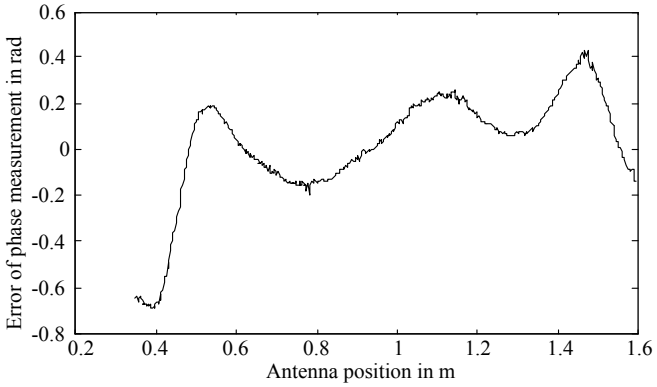

Figure 10. Deviation of measured phase to ideal simulated phase.

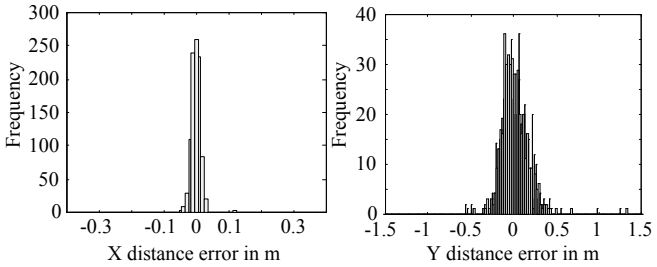

Figure 11. Probability of tag position errors in x- and y-direction.

the point of the antenna from which radiation emanates to form ideal spherical wave fronts. This is only possible if the phase center is a single point. For complex antenna patterns the phase center moves on the evolute of the equiphase wave front and can only be determined for small changes of the angle of sight. The effect of phase center displacement and a method of retrieving it are explained in [20]. To investigate the effect on the localization result in the presented measurement setup the phase distortion of the used standard antenna has been measured while turning it around its vertical axis. In the usual coordinates in spherical geometry the antenna was moved in the horizontal plane with constant elevation θ while varying the azimuth ϕ from 0 and π. The antenna has been turned counterclockwise. At $\pi/2$ the antenna is facing the tag. The result is shown in Fig. 12. The measured phase offset was approximated with a suitable best-fit curve. Utilizing this function the measurement data has been corrected. The original and the corrected data are shown in Fig. 13. The data shown in Fig. 13 was corrected with knowledge of the actual tag position which is necessary to calculate the angle of sight and retrieve a correction value. In contrast, the holographic image and the tag position was recalculated utilizing corrected phase data assuming the maximum calculated in section IV as the tag position. The maximum of the image moved slightly to $x_t = 0.96$ m and $y_t = 1.52$ m. Thus the distance error between the actual tag position and the measured positions decreases from 0.072 m to 0.063 m with the corrected phase data.

Antennas with a large beam width are favorable for holographic / synthetic aperture methods. If the antennas phase response is measured and taken into account, the correction will increase accuracy for those angles which are particularly valuable to determine the lateral position of the tag.

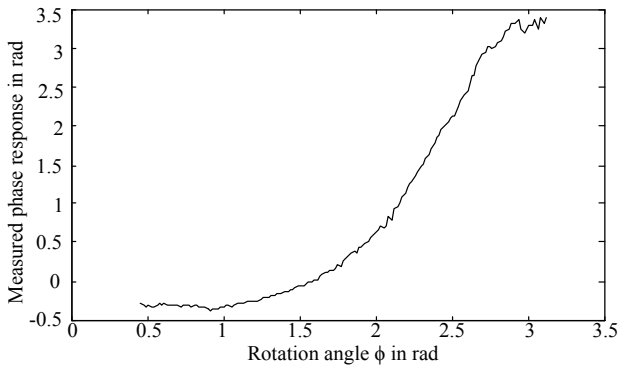

Figure 12. Measured antenna phase response in respect to the angle of sight.

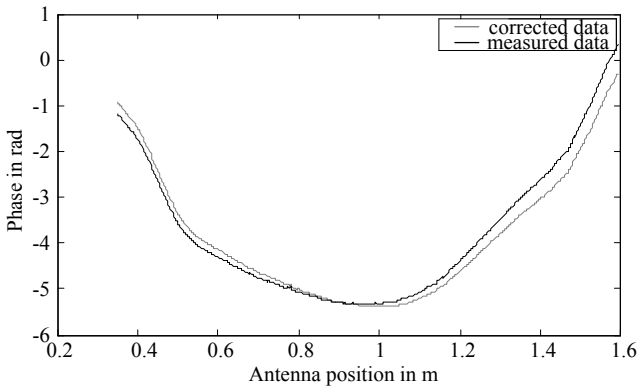

Figure 13. Measured and corrected phase data.

VII. CONCLUSION

A novel method for localization of standard Gen 2 UHF RFID tags has been presented. This method is easily applicable to any RFID reader providing phase readout. As shown, a synthetic aperture of roughly 0.3 m is sufficient to localize a tag with an uncertainty in the range of a decimeter even under indoor multipath conditions. Holographic localization comprises a substantial computational burden. This is especially true if a 3D localization is intended. We are currently working towards methods to identify a region of interest before the holographic localization is carried out. This way the computational effort can be reduced drastically. Different options to measure the antenna trajectory are also under investigation. Beside odometric sensors, reference transponders or the combination of inertial sensors and local positioning can be applied.

REFERENCES

[1] J. Heidrich, D. Brenk, J. Essel, S. Schwarzer, K. Seemann, G. Fischer, and R. Weigel, "The Roots, Rules, and Rise of RFID," *IEEE Microwave Magazine,* vol. 11, pp. 78-86, 2010.

[2] M. Vossiek, R. Miesen, and J. Wittwer, "RF identification and localization - recent steps towards the internet of things in metal production and processing," in *18th Intl. Conference on Microwave Radar and Wireless Communications (MIKON),* 2010, pp. 1-8.

[3] P. V. Nikitin, R. Martinez, S. Ramamurthy, H. Leland, G. Spiess, and K. V. S. Rao, "Phase based spatial identification of UHF RFID tags," in *2010 IEEE International Conference on RFID*, 2010, pp. 102-109.

[4] L. Xin, Z. Yimin, and M. G. Amin, "Multifrequency-based range estimation of RFID Tags," in *2009 IEEE International Conference on RFID*, 2009, pp. 147-154.

[5] D. Arnitz, K. Witrisal, and U. Muehlmann, "Multifrequency Continuous-Wave Radar Approach to Ranging in Passive UHF RFID," *IEEE Transactions on Microwave Theory and Techniques,* vol. 57, pp. 1398-1405, 2009.

[6] V. Viikari, P. Pursula, and K. Jaakkola, "Ranging of UHF RFID Tag Using Stepped Frequency Read-Out," *IEEE Sensors Journal,* vol. 10, pp. 1535-1539, 2010.

[7] M. Vossiek, R. Roskosch, and P. Heide, "Precise 3-D Object Position Tracking using FMCW Radar," in *29th European Microwave Conference,* 1999, pp. 234-237.

[8] J. Heidrich, D. Brenk, J. Essel, G. Fischer, R. Weigel, and S. Schwarzer, "Local positioning with passive UHF RFID transponders," in *2009 IEEE International Microwave Workshop on Wireless Sensing, Local Positioning, and RFID, IMWS 2009.* pp. 1-4.

[9] S. Kunkel, R. Bieber, H. Ming-Shih, and M. Vossiek, "A concept for infrastructure independent localization and augmented reality visualization of RFID tags," in *IEEE MTT-S International Microwave Workshop on Wireless Sensing, Local Positioning, and RFID, 2009. IMWS 2009.*, 2009, pp. 1-4.

[10] D. Arnitz, G. Adamiuk, U. Muehlmann, and K. Witrisal, "UWB channel sounding for ranging and positioning in passive UHF RFID," in *COST 2100 MCM*, Aalborg, DK, 2010.

[11] G. Hislop and C. Craeye, "Spatial smoothing for 2D direction finding with passive RFID tags," in *Antennas & Propagation Conference, 2009. LAPC 2009. Loughborough*, 2009, pp. 701-704.

[12] A. F. Mindikoglu and A. J. van der Veen, "Separation of overlapping RFID signals by antenna arrays," in *IEEE International Conference on Acoustics, Speech and Signal Processing, ICASSP 2008.*, 2008, pp. 2737-2740.

[13] H. Ermert and R. Karg, "Multifrequency Acoustical Holography," *Sonics and Ultrasonics, IEEE Transactions on,* vol. 26, pp. 279-285, 1979.

[14] M. Vossiek, Y. Magori, and H. Ermert, "An ultrasonic multielement sensor system for position invariant object identification," in *Proceedings of the 1994 IEEE Ultrasonics Symposium, IEEE*, 1994, pp. 1293-1297 vol.2.

[15] M. Younis, C. Fischer, and W. Wiesbeck, "Digital beamforming in SAR systems," *IEEE Transactions on Geoscience and Remote Sensing,* vol. 41, pp. 1735-1739, 2003.

[16] M. Vossiek, A. Urban, S. Max, and P. Gulden, "Inverse Synthetic Aperture Secondary Radar Concept for Precise Wireless Positioning," *IEEE Transactions on Microwave Theory and Techniques,* vol. 55, pp. 2447-2453, 2007.

[17] R. J. King, *Microwave Homodyne Systems*. London, U.K.: Peregrinus, 1978.

[18] P. Heide, et. al., US Patent US6946949B2, November 30, 2000.

[19] T. Nowak and A. Eidloth, "Dynamic multipath mitigation applying unscented Kalman Filters in local positioning systems," in *2010 European Wireless Technology Conference (EuWIT)* , 2010, pp. 9-12.

[20] S. R. Best, "Distance-measurement error associated with antenna phase-center displacement in time-reference radio positioning systems," *IEEE Antennas and Propagation Magazine,* vol. 46, pp. 13-22, 2004.